Light emission from silicon/gold nanoparticle systems

M. Bassu,[1,a)] M. L. Strambini,[1] G. Barillaro,[1] and F. Fuso[1,2]
[1]*Dipartimento di Ingegneria dell'Informzione, Universitá di Pisa, via G. Caruso 16, 56122 Pisa, Italy*
[2]*Dipartimento di Fisica Enrico Fermi, Università di Pisa, Largo Bruno Pontecorvo 3, 56127 Pisa, Italy*

(Received 25 June 2010; accepted 3 August 2010; published online 7 October 2010)

Photoluminescent nanostructured semiconductor/metal systems consisting of silicon nanocrystals and gold nanoparticles are obtained by gold-catalyzed chemical etching. The interplay between silicon and gold nanostructures is investigated by photoluminescence spectroscopy upon continuous and pulsed excitation, both at room and low temperature. Comparison with reference samples, obtained removing gold particles by selective etching, highlights an enhanced emission in samples containing silicon and gold nanoparticles, explained in terms of both surface modifications and optical coupling between emitting nanocrystals and nanoparticles featuring localized plasmon resonances. © *2010 American Institute of Physics*. [doi:10.1063/1.3483617]

There is presently a growing interest in coupled systems consisting of semiconductor nanocrystals (NCs) and metal nanoparticles (NPs), or nanostructured metal surfaces. Interaction with NPs can actually represent a viable route to modify the spectral features of the NCs and to improve the emission efficiency, providing in addition with a handle useful to interact with the semiconductor in terms of both electron injection (see, e.g., pore filling with metals[1]) and light manipulation in integrated plasmonics devices.[2] The ability of noble metal nanostructures to rule the optical properties of Si has been already demonstrated, and a remarkable enhancement of the radiative emission rates has been observed.[3] The unique properties of roughened metal surface or NPs, made of gold, silver, copper, and platinum,[4–6] have been intensively studied over the past decades. Au nanostructures exhibits peculiar absorption peaks[7] at visible wavelengths due to surface plasmon (SP) resonances. Whenever the plasmon resonance, whose wavelength is ruled by NP size and shape, and by the refractive index of the external medium, falls within the NC emission spectrum, an optically coupled system can be formed leading to peculiar interplay effects.

In this letter, we report on the optical properties of porous silicon (PS) samples obtained using a process similar to the H_2O_2 metal HF (HOME-HF) etching technique,[8] based on Au NPs assisted chemical etching of Si substrates. Systems consisting of Si NCs and Au NPs are inherently produced in a single-step process. Sample photoluminescence (PL) is investigated upon continuous wave (cw) and pulsed wave excitation, both at room and low temperature; comparison is made with gold-free samples, i.e., similarly grown samples with Au removed through wet etching.

Samples were produced in different conditions and starting from different materials (both n and p doped Si wafer). Here we will restrict to samples prepared from MEMC ⟨100⟩ p-type Si ($N_A = 0.5-1\times10^{15}$ cm^{-3}). Buffered HF etching is performed on the wafer in order to obtain an hydrogen terminated and oxide free Si surface. A 10 nm thick Au film is deposited by thermal evaporation of Au onto the silicon wafer in a residual pressure of 2×10^{-6} mbar. After gold deposition the sample is placed into a rapid thermal annealing (RTA) chamber (JIPELEC JET FIRST 100) and is annealed for 240 s at 1000 °C in N_2 purging.

In the RTA process, Au may diffuse into the Si substrate to form alloy at the interface.[9] Inter atomic interaction and strong surface tension lead to spherical Au–Si liquid droplets on the substrate giving rise, after cooling, to Au NPs on the wafer surface. Typical morphology and size distribution of the so-produced NPs are shown in the scanning electron microscope (SEM) images of Figs. 1(a) and 1(b), demonstrating a roughly spherical shape with most probable diameters around 60–80 nm. The sample is then etched in a HF (48%) and H_2O_2 (30%) solution (1:10 in volume) for 15 min.

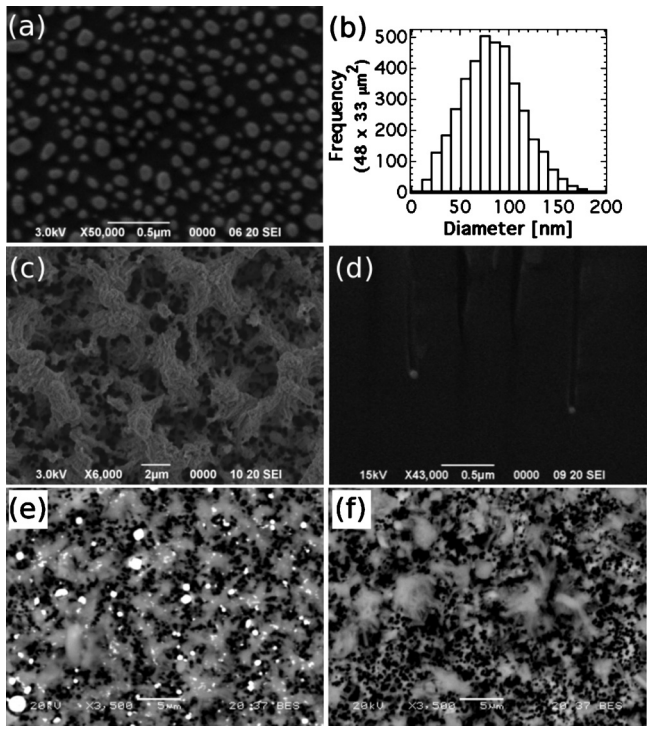

FIG. 1. SEM plan view of the NPs produced on Si according to the process described in the text (a); size distribution of the NPs found on a 48 $\times$33 μm^2 area (b); SEM plan view and cross section of a PSAu sample [(c) and (d), respectively]; BSE images of a PSAu (e) and of a PSAuE (f) sample: white spots in the image (e) are associated with the presence of Au, and their absence in image (f) demonstrates efficient Au etching.

a)Electronic mail: margherita.bassu@iet.unipi.it.

The NPs act as reaction mediators promoting Si dissolution without the need of an external bias.[10] The morphology of the etched layer features the presence of two different sub layers, as shown in Figs. 1(c) and 1(d). The first one, given by the initial random motion of Au NPs due to the contact with the etchant solution, is superposed to the second one, which appears composed by an almost regular sequence of ~8 μm depth pores with Au NPs at the bottom.

As prepared samples are cut in two parts and a selective Au removal is performed on one of them through 15 min etching in a solution obtained by mixing 200 ml of H_2O, 340 g of KI, and 7 g of I_2. Removal of Au is intended to produce reference samples with morphology similar to the original (NP-containing) one but without Au. The two samples, denoted hereafter as PSAu and PSAuE, respectively, were analyzed using the back-scattered electron (BSE) mode of a SEM, which confirms removal of Au NPs without apparent morphological modifications, as shown in Figs. 1(e) and 1(f).

PL spectra were acquired upon cw (λ=405 nm) and pulsed excitation (λ=308 nm, pulse duration ~17 ns, repetition rate 13 Hz), and measured in the visible-near IR range by a photomultiplier mounted at the output of a monochromator; data have been corrected for the spectral response of the system. In both cases, the laser beam has been shaped to a 1 mm^2 spot and the intensity kept well below the damage, or ablation, threshold of the material (actual intensity <0.1 mW/cm^2 and fluence <10 mJ/cm^2 in the cw and pulsed experiments, respectively). In time resolved analysis, decay traces were recorded for every wavelength and time integrated spectra were obtained by software-based boxcar integration of the signal between 0.7 and 95 μs after the arrival of the laser pulse, a time interval chosen to minimize contribution from scattering of the laser pulse and to account for the whole emission dynamics from the samples. Low temperature investigations have been carried out by cooling the samples (down to ~50 K) in an evacuated He-closed cycle cryostat.

Under laser illumination, PSAu samples emit an intense orange light easily visible to the naked eye. Remarkably, in all investigated samples PL intensity of PSAu was found larger than in the corresponding PSAuE samples, being such enhancement accompanied with a redshift in several tens of nanometer. Interestingly PL is rather stable and unaffected by exposure to air: we observed similar PL spectra and maximum intensity in as-grown samples (analysis carried out roughly 10 h after the preparation) and in samples stored for several months in air. Typical PL spectra from PSAu and PSAuE samples are reported in Fig. 2(a) upon cw and pulsed excitation (continuous and dashed lines, respectively). PL appears blue shifted when pulsed excitation is used, which can be explained by considering the higher photon energy (E_{phot}~4 eV and 3 eV, for pulsed and cw excitation, respectively). The PL enhancement factor for the NP-containing sample is around 3 in both cases, measured at the peak wavelength of the spectra. The time resolved PL signal is well reproduced by a double exponential function with τ_1 and τ_2, "long" and "short" lifetimes, respectively. The short lifetime is about 1.5 μs for both PSAu and PSAuE samples. On the contrary, the long lifetime, determining the overall decay rate, depends on the presence of the Au NPs. For the reference sample (PSAuE) τ_1=6.1 μs at the peak wavelength,

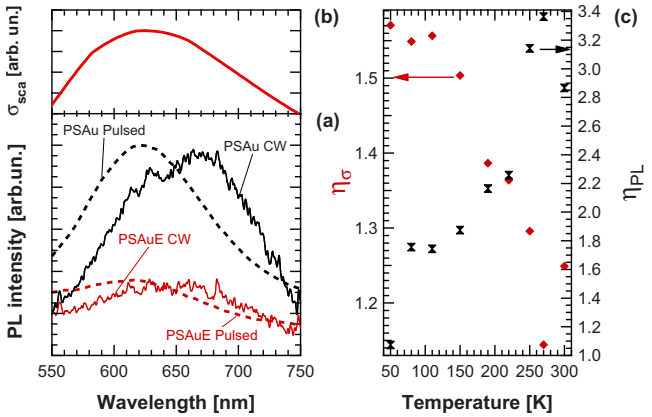

FIG. 2. (Color online) Typical PL spectra for PSAuE and PSAu samples upon cw and pulsed excitation, the latter being time-integrated over the whole duration of the PL decay (a). Calculated spectrum of the plasmon scattering for NPs in conditions similar to our experiment (b). Effective excitation cross section enhancement, η_σ at 635 nm, and η_{PL} as a function of the temperature (c).

whereas τ_1=18 μs for the coupled (PSAu) sample. This result is in disagreement with observations reported by other groups,[3,11] where PL decay rates are shown to be increased by electron-hole pair or exciton–SP coupling rate $\Gamma_{SP}=1/\tau_{SP}$, expected to be very fast. On the other hand, Liu *et al.*[12] have observed PL enhancement for a ZnO light emitting thin film coupled with a noble metal nanopattern, accompanied with a slowing down of the decay. In that work, surface modifications associated with the presence of the metal nanopattern, and the consequent alteration of the defective sites acting as nonradiative recombination centers, were claimed to govern the observed behavior. Such an alteration can play relevant role when PL is dominated by nonradiative recombination, that is the case, besides ZnO, of PS.[13]

Temperature resolved analysis, carried out upon pulsed excitation, can help in assessing the role of different de-excitation processes. For PSAuE, a slight decrease in both PL and τ_1 was observed as the temperature decreases. This suggests negligible coupling with substrate phonons. On the contrary, the PsAu shows a comparatively larger dependence on the temperature for both lifetime and intensity. In particular, τ_1 decreases by one order of magnitude from room temperature to 50 K, and the time-averaged peak intensity decreases roughly by a factor two.

Radiative energy exchange between NCs and NPs is expected as well. We can estimate the spectrum of the localized plasmon scattering by the Au NPs embedded in the porous matrix according to the Mie model. Calculations have been performed with the MIEPLOT code,[14] using the size distribution obtained from SEM analysis and the refractive index obtained by the Bruggeman formula,[15] assuming a Si porosity around 50%, compatible with our sample morphology. The calculated resonance spectrum, shown in Fig. 2(b), overlaps substantially with measured PL. Radiative coupling is enhanced in the near-field, i.e., in the vicinity of the NP surface, through the occurrence of local field enhancement, therefore it requires NPs to be close, at a distance $\leq$10 nm, to the Si emitting centers. Thanks to the NP-catalyzed etching, the requirement is likely to be satisfied in our samples. We can thus envision interaction processes where energy is exchanged between NCs, directly excited by the laser radiation, and NPs; extraction of such a radiative energy in the

far-field involves resonant scattering from NPs.

Upon pulsed excitation, the PL spectrum turns affected by the choice of the time integration window. In particular, the shorter the window, the more intense is the blue component of the spectrum. Such a behavior, typical of PS produced by anodization,[16] can be related to the different decay dynamics experienced by the emitting centers contributing to the blue emission. PS grown with metal-assisted chemical etching is shown in the literature to exhibit remarkable blue PL.[17] We observe blue-shifted spectra when boxcar averaging is performed over the fast decay time τ_2. We note, that no enhancement of the fast, blue, component is observed in PSAu, suggesting that emission enhancement occurs only for those wavelengths within the localized plasmon resonance range.

The PL decay rate $\Gamma_{\mathrm{exp}}^{(\mathrm{PSAuE})}$ measured in PSAuE samples can be expressed as

$$\Gamma_{\mathrm{exp}}^{(\mathrm{PSAuE})} = \Gamma_{\mathrm{R}} + \Gamma_{\mathrm{NR}}, \tag{1}$$

being Γ_{R} and Γ_{NR} the radiative and nonradiative rates, respectively. The PL decay rate $\Gamma_{\mathrm{exp}}^{(\mathrm{PSAu})}$ in PSAu samples can be expressed as

$$\Gamma_{\mathrm{exp}}^{(\mathrm{PSAu})} = \Gamma_{\mathrm{R}} + \Gamma_{\mathrm{NR}}^{*} + \Gamma^{(P)}, \tag{2}$$

where Γ_{NR}^{*} is the altered nonradiative decay rate, including surface modification effects, and $\Gamma^{(P)}$ is the rate of coupling with localized plasmon resonances, which, due to the near-field nature of the coupling, is expected to be strongly dependent on the distance between NCs and NPs.[18] $\Gamma^{(P)}$ can in turn be divided into radiative and nonradiative components, the latter involving for instance dissipation of plasmon excitation.[19] The radiative coupling between NCs and NPs can affect the excitation cross section as well. In fact part of the exciting laser energy can be transferred to NPs, acting as some kind of a leakage channel for the NC excitation. On the other hand, modifications of the density of states of the exciton system in the NC can occur due to local interaction with metal NPs, leading to cross section enhancement.[20] The parameters ruling the process can be estimated by analyzing the growing portion of the time-resolved PL signal, after due deconvolution for the temporal response of the detection system and for direct scattering of the laser shot. We have estimated the PL rise time τ_{on} (the $1/e$ time for the PL intensity to reach its saturation value, averaged over a large number of laser pulses in order to reduce statistical fluctuations), and the effective excitation cross section σ (Ref. 3) according to

$$\sigma\phi = \frac{1}{\tau_{\mathrm{on}}} + \Gamma_{\mathrm{exp}}, \tag{3}$$

where ϕ is the photon flux in the laser excitation pulse. Despite of the limited temporal resolution of our apparatus, we have systematically found σ values larger in the PSAu than in the PSAuE samples. Figure 2(c) shows (rhombus) the effective excitation cross section enhancement $\eta_\sigma = \sigma_{(\mathrm{PSAu})}/\sigma_{(\mathrm{PSAuE})}$ as a function of the temperature, and the PL intensity enhancement factor $\eta_{\mathrm{PL}} = I_{\mathrm{PL}}^{\mathrm{PSAu}}/I_{\mathrm{PL}}^{\mathrm{PSAuE}}$ (butterflies), i.e., the ratio between the time-integrated emission yield at the PL spectra peak in samples featuring, or not, Au NPs. Both quantities are greater than one in the whole explored temperature range. However, the behavior is markedly different, being either increasing or decreasing when the temperature decreases for η_σ or η_{PL}.

Two different materials are present in the porous layer, with different thermal coefficients (for reference, the expansion coefficient in bulk and room temperature is larger by a factor 3 for Au with respect to Si). Au NPs may for instance undergo thermal contraction upon cooling, that can even lead, in case of nanosized structures, to modify the optical properties.[21,22] Temperature-induced mechanical variations, possibly amplified by stress in the porous structure where NPs sit, can lead to modify the average distance between NC and NP. Biteen *et al.*[3] have demonstrated that for an average distance change as small as several nm the near-field coupling efficiency is strongly modified. In particular, a correlated behavior between η_σ and η_{PL}, as a function of distance has been found. On the contrary, our results point out on anti-correlation between the two trends. A possible explanation can be found in the already mentioned nonradiative deexcitation occurring at the Au NPs. In our samples the nonradiative rate $\Gamma_{\mathrm{NR}}^{(P)}$ increases as a function of the temperature more rapidly than the radiative counterpart, $\Gamma_{\mathrm{R}}^{(P)}$. This hypothesis can also explain the observed behavior of τ_1, decreasing along with the PL intensity.

Our results show that also at room temperature integration of noble metal NPs with Si NCs in a porous environment, can effectively lead to emission efficiency improvement. Such integration can have additional appealing outcomes from the point of view of fabrication. Further work will be devoted to understand the local mechanisms involved in the optical interaction between NCs and NPs by using near-field optical microscopy and to investigate the electronic properties of the coupled system in view of practical exploitations in optoelectronics.

[1] J.-Y. Yoon, M.-S. Kim, J.-Y. Lee, and J.-H. Yoon, Nanotechnology **16**, 1372 (2005).
[2] A. Alqudami and S. Annapoorni, Plasmonics **2**, 5 (2007).
[3] J. S. Biteen, D. Pacifici, N. S. Lewis, and H. A. Atwater, Nano Lett. **5**, 1768 (2005).
[4] R. P. Devaty and A. J. Sievers, Phys. Rev. B **31**, 2427 (1985).
[5] S.-K. Eah, H. M. Jaeger, N. F. Scherer, G. P. Wiederrecht, and X.-M. Lin, Appl. Phys. Lett. **86**, 031902 (2005).
[6] C. Langhammer, Z. Yuan, I. Zorić, and B. Kasemo, Nano Lett. **6**, 833 (2006).
[7] M. M. Alvarez, J. T. Khoury, T. G. Schaaff, M. N. Shafigullin, I. Vezmar, and R. L. Whetten, J. Phys. Chem. B **101**, 3706 (1997).
[8] X. Li and P. W. Bohn, Appl. Phys. Lett. **77**, 2572 (2000).
[9] N. Ferralis, R. Maboudian, and C. Carraro, J. Am. Chem. Soc. **130**, 2681 (2008).
[10] S. Chattopadhyay, X. Li, and P. W. Bohn, J. Appl. Phys. **91**, 6134 (2002).
[11] X. Hu, Y. Huang, W. Zhang, and J. Peng, Appl. Phys. Lett. **89**, 081112 (2006).
[12] K. W. Liu, Y. D. Tang, C. X. Cong, T. C. Sum, A. C. H. Huan, Z. X. Shen, L. Wang, F. Y. Jiang, X. W. Sun, and H. D. Sun, Appl. Phys. Lett. **94**, 151102 (2009).
[13] H. Koyama, T. Ozali, and N. Koshida, Phys. Rev. B **52**, R11561 (1995).
[14] www.philiplaven.com.
[15] W. Theiß, S. Henkel, and M. Arntzen, Thin Solid Films **255**, 177 (1995).
[16] Z. Łukasiak, P. Dalasiński, and W. Bała, Opto-Electron. Rev. **11**, 113 (2003).
[17] T. Hadjersi, N. Gabouze, N. Yamamoto, C. Bennazzouz, and H. Cheraga, Vacuum **80**, 366 (2005).
[18] J. Gersten and A. Nitzan, J. Chem. Phys. **75**, 1139 (1981).
[19] R. Carminati, J.-J. Greffet, C. Henkel, and J. M. Vigoureux, Opt. Commun. **261**, 368 (2006).
[20] D. Kovalev, J. Diener, H. Hecker, G. Polisski, N. Künzner, and F. Koch, Phys. Rev. B **61**, 4485 (2000).
[21] W.-H. Li, S. Y. Wu, C. C. Yang, S. K. Lai, K. C. Lee, H. L. Huang, and H. D. Yang, Phys. Rev. Lett. **89**, 135504 (2002).
[22] W.-H. Li, S. Y. Wu, C. C. Yang, F. C. Tsao, S. K. Lai, and K. C. Lee, Synth. Met. **135–136**, 811 (2003).